KINETICS

The Law of Mass Action

In the case of reacting systems,

$$aA + bB \rightleftharpoons cC + dD$$

where *a, b, c, and d are the stoichiometric coefficients of species A, B, C, and D* generically represented by ν_i

stoichiometric coefficients are positive for products and negative for reactants

The *Law of Mass Action states that the velocity of the reaction at a given temperature*is proportional to the product of the active masses of the reacting substances.

$$r_1 = k_1[A]^a[B]^b$$

$$r_2 = k_2[C]^c[D]^d$$

At equilibrium, $\Delta G = 0$ and $r_1 = r_2$

Equilibrium constant $K = \frac{k_1}{k_2} = \frac{[C]^c[D]^d}{[A]^a[B]^b}$

The free energy of a system is simply the sum of the free energy contributions of each of the components measured using chemical potentials

$$\Delta G = \sum \nu_i \mu_i$$

When all the components are in their standard states the standard Gibbs free energy, ΔG_0, *is given by:*

$$\Delta G^0 = \sum \nu_i \mu_i^0$$

Now, $\mu_i = \mu_i^0 + RT \ln a_i$

$$\Delta G - \Delta G^0 = RT \sum \nu_i \ln a_i = RT \ln \left(\prod_i a_i^{\nu_i} \right)$$

At equilibrium, then, $\Delta G = 0$, *and the activities of the products and reactants,* a_i, *are* related to their respective concentrations:

$$\Delta G^o = -RT \ln \left\{ \frac{[C]^c [D]^d}{[A]^a [B]^b} \right\}$$

Thus, $$\Delta G^0 = -RT \ln K$$

$$K = \exp \left(\frac{-\Delta G^0}{RT} \right)$$

Both k_1 and k_2 can also be expressed as:

$$k = k_0 \exp(-E_a / RT)$$

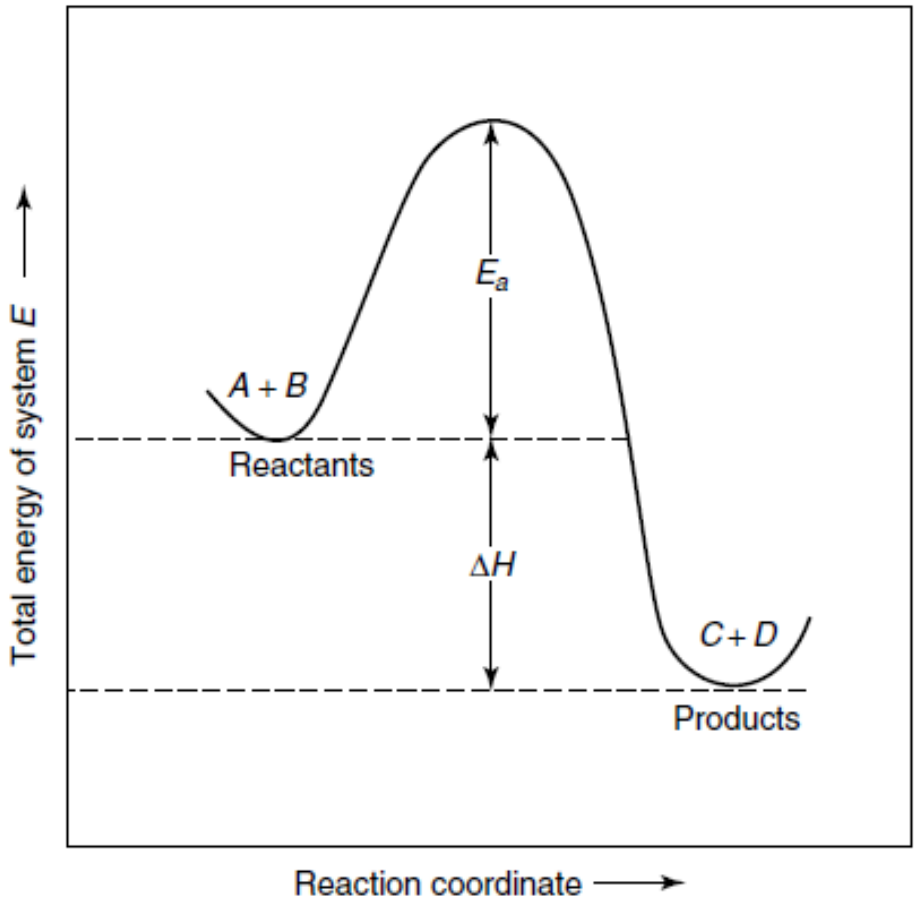

Figure 3.1 Activation energy barrier for a chemical reaction.

ΔH is the heat of reaction and may be negative (exothermic)or positive (endothermic)

Kinetics of Inter-metallic Formation

Dissolution of Ti in molten aluminum to form the inter-metallic $TiAl_3$

Temperature (°C)	Rate of Ti Dissolution, k_{Ti} (cm/s)	Rate of $TiAl_3$ Formation, k_{TiAl_3} (cm/s)
700	1.51×10^{-6}	1.042×10^{-5}
750	2.605×10^{-6}	1.98×10^{-5}
800	4.17×10^{-6}	2.777×10^{-5}
850	6.13×10^{-6}	3.798×10^{-5}
900	9.36×10^{-6}	6.805×10^{-5}

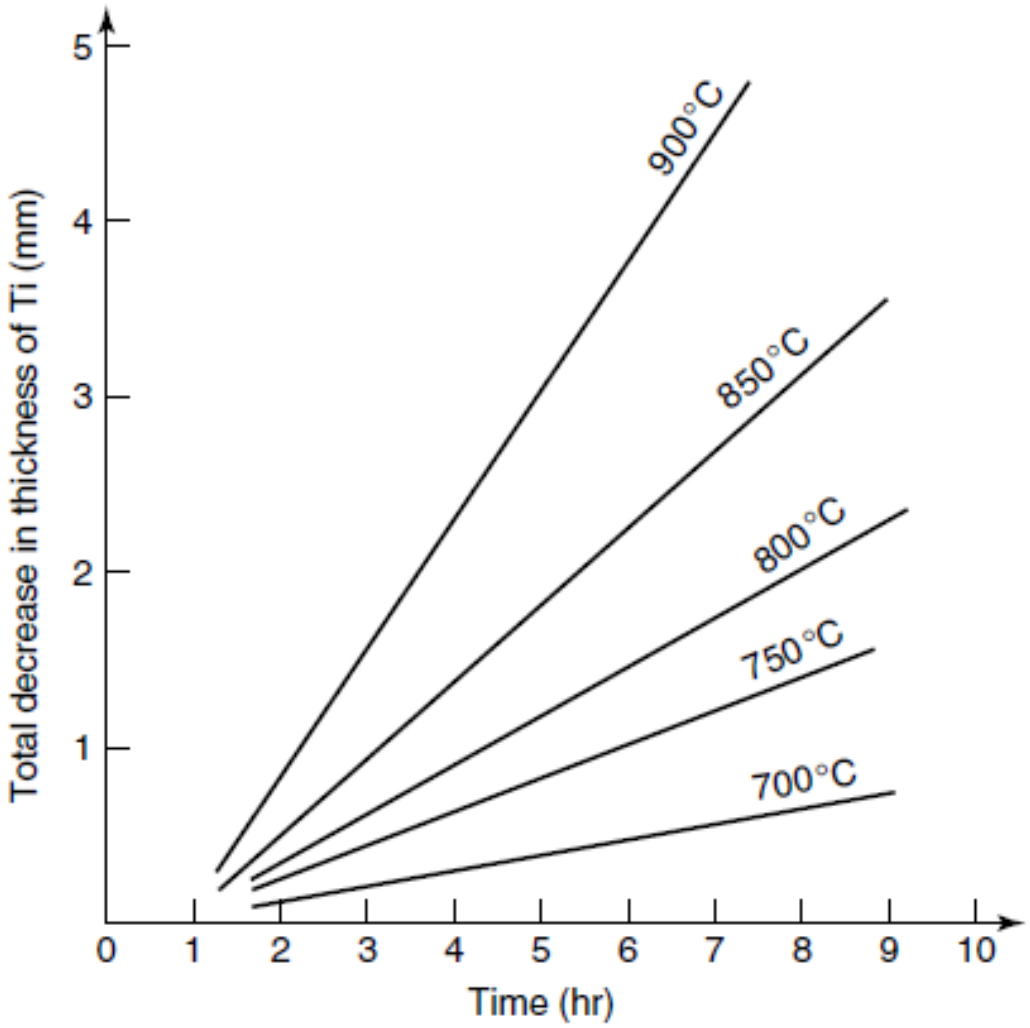

Figure 3.2 Rate of dissolution of Ti at various temperatures.

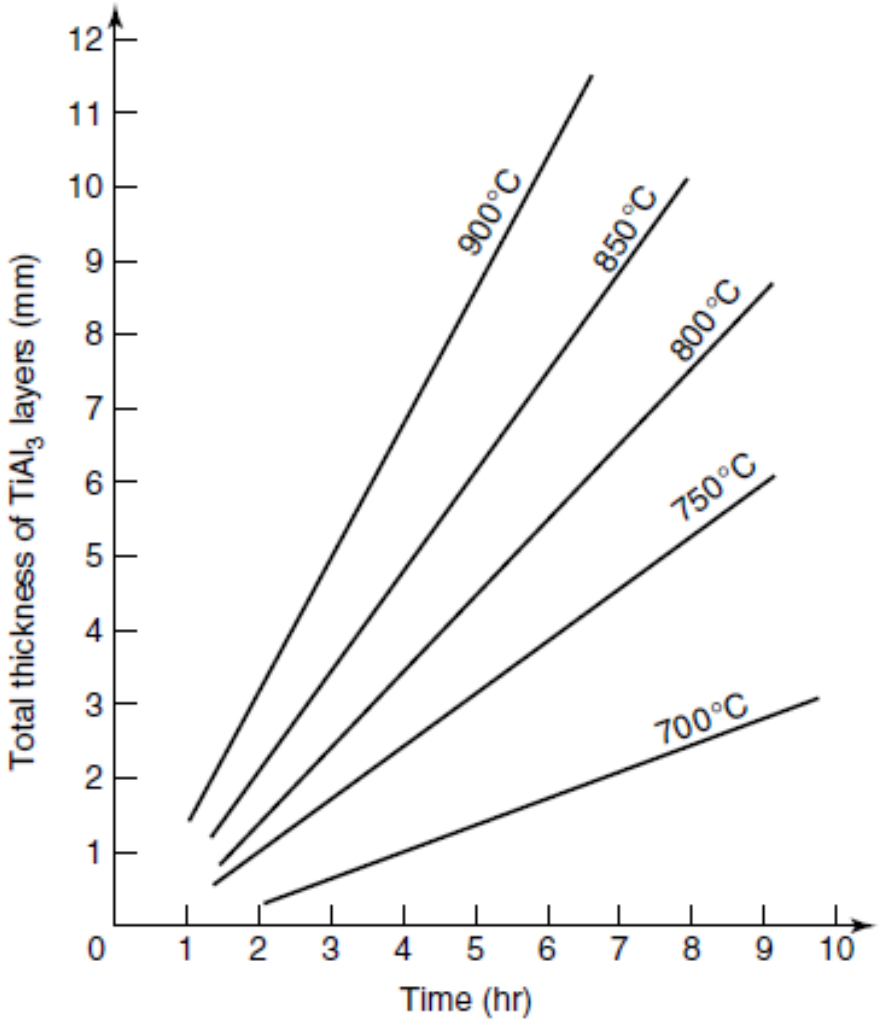

Figure 3.3 Rate of formation of $TiAl_3$ at various temperatures.

$$E_{a,Ti} = 86 \text{ kJ/mol}; \; k_{0,Ti} = 0.06$$

$$E_{a,TiAl_3} = 84 \text{ kJ/mol}; \; k_{0,TiAl_3} = 5.3$$

The fact that the two activation energies calculated are essentially equivalent tells us that the rate of the chemical reaction between these two metals, and not the diffusion of either aluminum or titanium through the intermetallic layer formed on the surface of the solid titanium determines the overall rate of $TiAl_3$ formation.

Kinetics of Phase Transformations in Metals and Alloys

Crystallization or *devitrification process*
Amorphous or glassy solid → *crystallization*

Isothermal case

$$\frac{dx}{dt} = nk(1-x)t^{n-1}$$

Solution: $$x = 1 - \exp[-kt^n]$$

Johnson–Mehl–Avrami (JMA) equation

Taking the natural log of this equation twice

$$\ln[-\ln(1-x)] = \ln k + n \ln t$$

Table 3.1 Values of the Growth Dimension, n (a.k.a Reaction Order), for Different Crystallization Processes

Mechanism	n
Bulk nucleation, 3-dimensional growth	4
Bulk nucleation, 2-dimensional growth	3
Bulk nucleation, 1-dimensional growth	2
Surface nucleation	1

Non-isothermal case

1) $$\ln[-\ln(1-x)] = n\ln\phi + \ln k + \text{constant}$$

φ is the heating rate, *usually in K/min,*

2) $$\ln\left(\frac{\phi}{T_p^2}\right) = \text{constant} - \frac{E_a}{RT_p}$$

T_p is the temperature at which the transformation rate is a maximum
Determined from DSC or DTA

KINETIC PROCESSES IN CERAMICS AND GLASSES

Consider solidification from melt
L → S transformation

At T_m:

$$\Delta G_v = \Delta H_f - T_m \Delta S_f = 0$$

ΔG_v is the free energy change per unit volume for fusion, ΔH_f is the enthalpy of fusion and *ΔS_f is the entropy of fusion*

$$\Delta S_f = \frac{\Delta H_f}{T_m}$$

Assuming that the entropy and enthalpy are relatively independent of temperature

$$\Delta G_v = \Delta H_f \left[\frac{(T_m - T)}{T_m} \right]$$

NUCLEATION

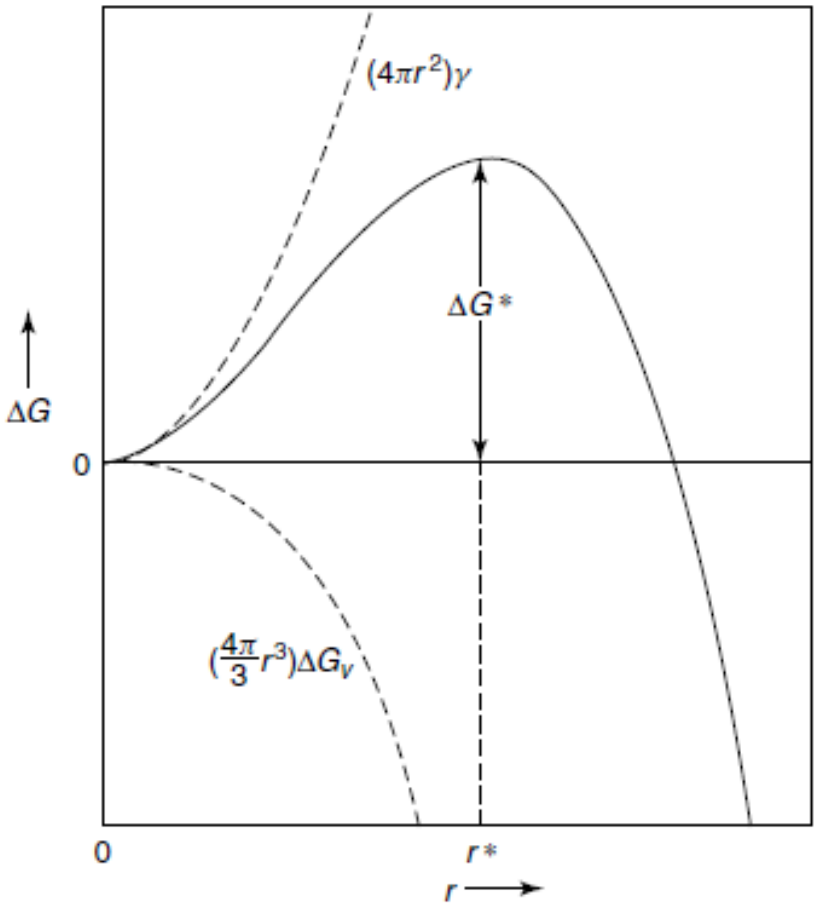

Figure 3.12 Representation of activation energy barrier for nucleation. From K. M. Ralls, T. H. Courtney, and J. Wulff, *Introduction to Materials Science and Engineering*. Copyright © 1976 by John Wiley & Sons, Inc. This material is used by permission John Wiley & Sons, Inc.

HOMOGENEOUS NUCLEATION

$$\left(\frac{4\pi r^3}{3}\right)\Delta G_v \qquad\qquad 4\pi r^2\gamma$$

$$\Delta G = \left(\frac{4\pi r^3}{3}\right)\Delta G_v + 4\pi r^2\gamma$$

$$r^* = \frac{-2\gamma}{\Delta G_v}$$

$$\Delta G^* = \frac{16\pi\gamma^3}{3\Delta G_v^2}$$

Heterogeneous nucleation

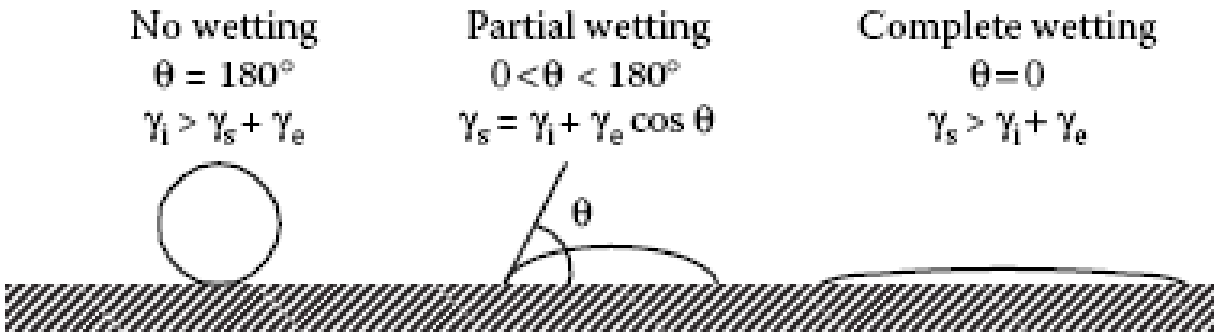

FIGURE 4.7
Wetting of a flat substrate by an epitaxial deposit. (Adapted from Ghandhi, S.K., *VLSI Fabrication Principles, Silicon and Gallium Arsenide*, 2nd ed., Wiley, New York, 1994. With permission.)

$$\gamma_s = \gamma_i + \gamma_e \cos\theta$$

$$\theta = \cos^{-1}\left(\frac{\gamma_s - \gamma_i}{\gamma_e}\right)$$

$$\Delta G = \frac{\pi r^3}{3}(1-\cos\theta)^2(2+\cos\theta)\Delta G_v + \pi r^2(\gamma_i - \gamma_s)\sin^2\theta + 2\pi r^2(1-\cos\theta)\gamma_e$$

$$\Delta G^*_{het} = \Delta G^*_{\text{hom}o}\left[\frac{(2+\cos\theta)(1+\cos\theta)^2}{4}\right]$$

$$\Delta G^*_{het} = \frac{16\pi\gamma_e^3(2+\cos\theta)(1-\cos\theta)^2}{12\Delta G_v^2}$$

$$\mathbb{N} = \nu n_s n^*$$

where $\mathbb{N}$ *is the number of critical nuclei that form per unit volume per unit time,*
n_s *is* the number of molecules in contact with critical nucleus,
n^* *is the number of critical* size clusters per unit volume, and
v is the collision frequency of single molecules with the nuclei

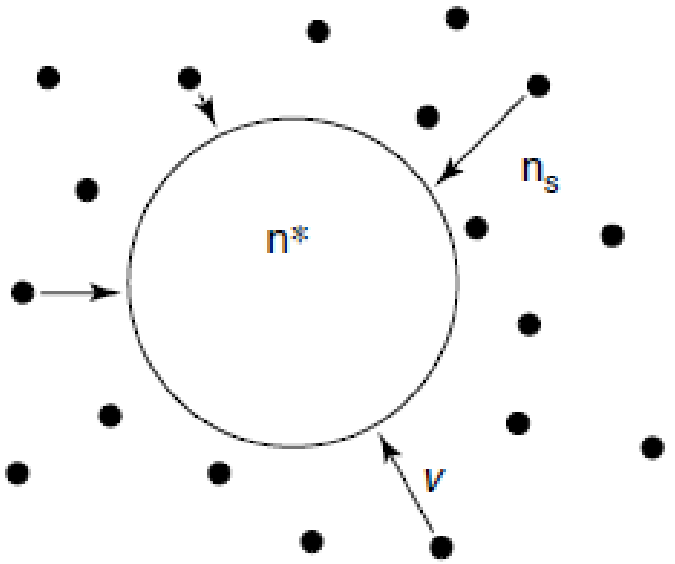

Figure 3.14 Schematic illustration of a nucleation site formation.

$$n^* = n_0 \exp(-\Delta G^* / k_B T)$$

where n_0 *is the number of single molecules per unit volume,*
k_B *is Boltzmann's constant,*
and *T is absolute temperature.*

$$\nu = \nu_0 \exp(-\Delta G_m / k_B T)$$

where ν_0 *is the molecular jump frequency,*
and G_m *is the activation energy for* transport across the nucleus–matrix interface

For homogeneous nucleation

$$\mathbb{N} = \nu_0 n_s n_0 \exp(-\Delta G^* / k_B T) \exp(-\Delta G_m / k_B T)$$

For heterogeneous nucleation

$$\mathbb{N} = \nu_0 n_s n_0 \exp(-\Delta G_s^* / k_B T) \exp(-\Delta G_m / k_B T)$$

Recall

$$\Delta G^* = \frac{16\pi\gamma^3}{3(\Delta G_v)^2}$$

Also

$$\Delta G_v = \frac{\Delta H_v(T_m - T)}{T_m}$$

$$\mathbb{N} = \nu_0 n_s n_0 \exp\left[\frac{-16\pi\gamma^3 T_m^2}{3k_B T \Delta H_v^2 (T_m - T)^2}\right] \exp\left(\frac{-\Delta G_m}{k_B T}\right)$$

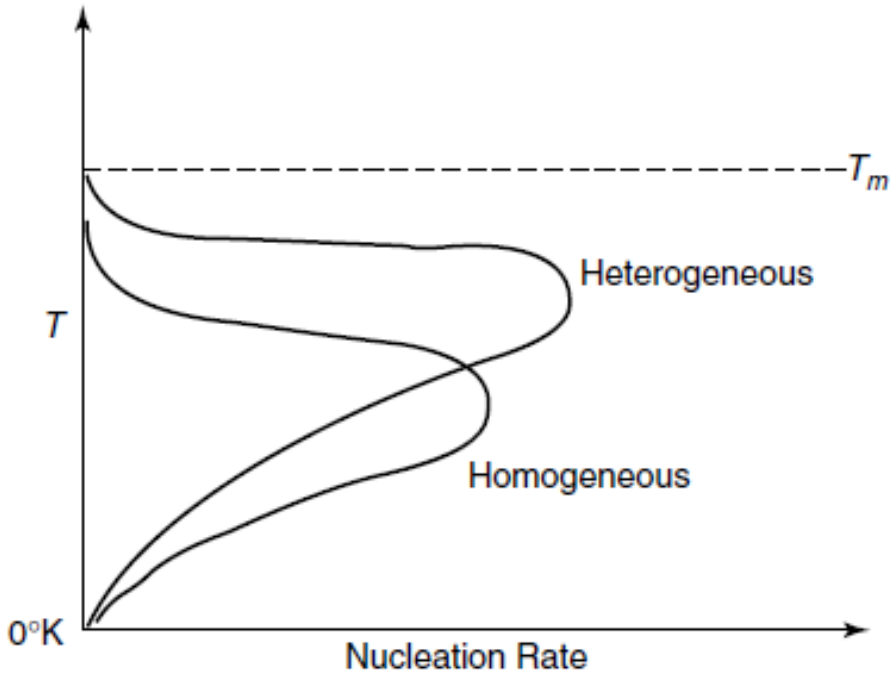

Figure 3.15 Effects of temperature and undercooling on homogeneous and heterogeneous nucleation rates.

GROWTH

- thermally activated (diffusion controlled)
- diffusionless (martensitic) - already discussed

thermally activated

$$\mathbb{R} = A[1 - \exp(\Delta G / k_{\mathrm{B}} T)]$$

The form of the preexponential factor, *A, depends on the type of theory*

OVERALL PHASE TRANSFORMATION RATE

$$\mathbb{P} = \mathbb{N} \times \mathbb{R}$$

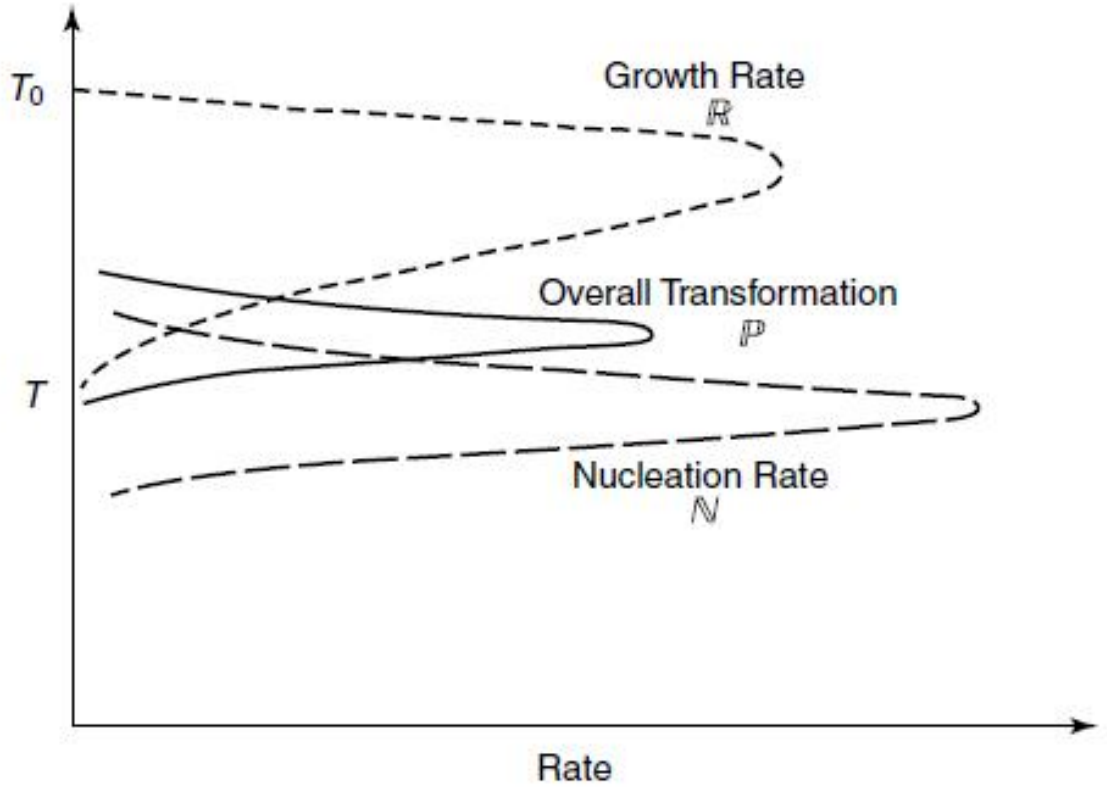

Figure 3.16 Schematic representation of transformation rates involved in crystallization by nucleation and growth kinetics.

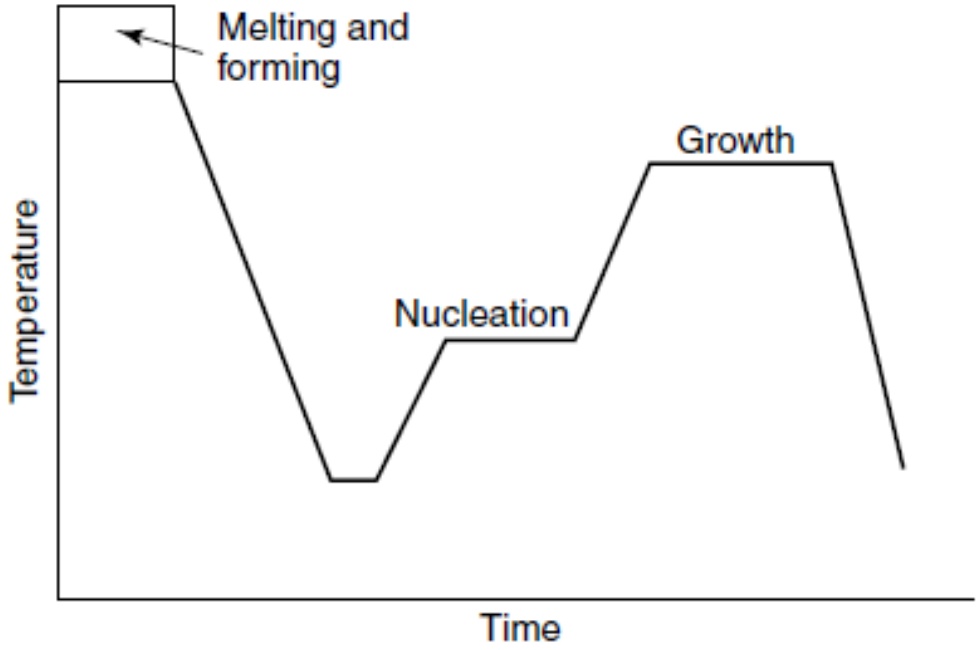

Figure 3.17 Schematic time-temperature cycle for the controlled crystallization of a glass-ceramic body.

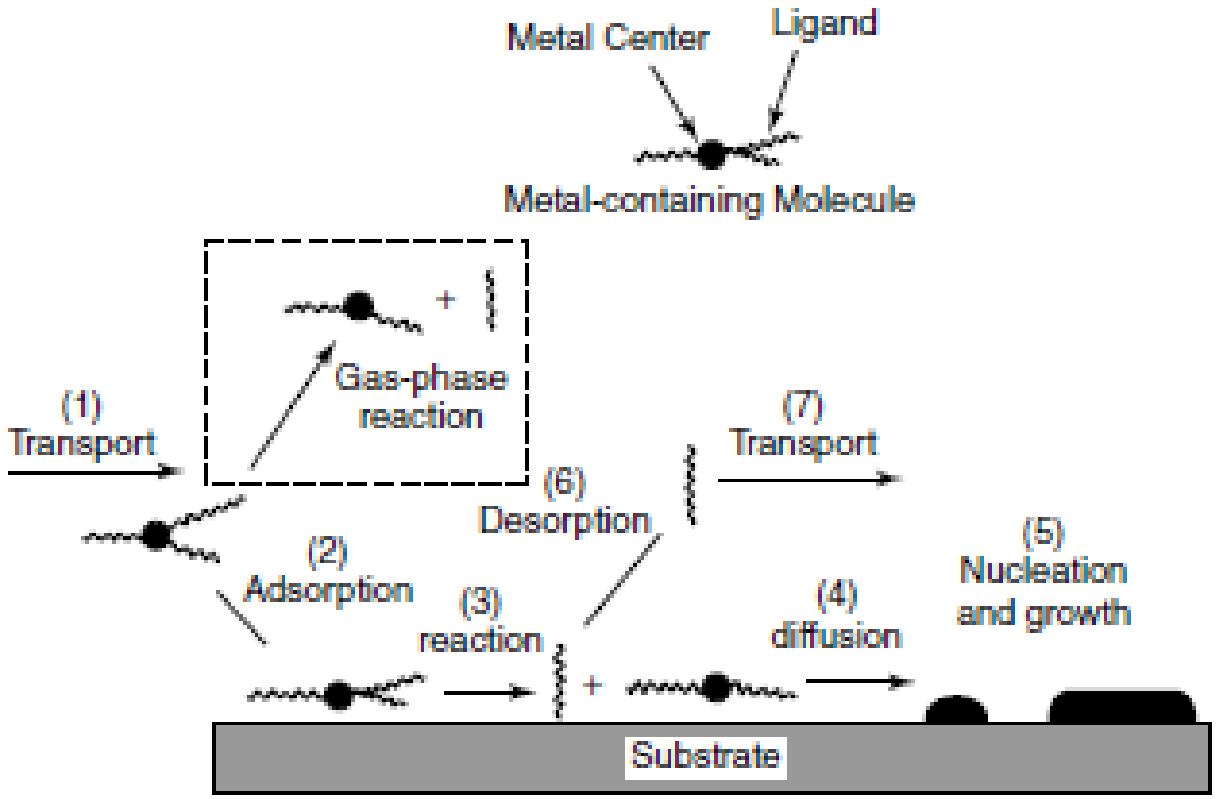

Figure 3.32 Processes involved in chemical vapor deposition. From *Chemistry of Advanced Materials: An Overview*, L. V. Interrante and M. J. Hampden-Smith, eds. Copyright © 1998 by John Wiley & Sons, Inc. This material is used by permission of John Wiley & Sons, Inc.

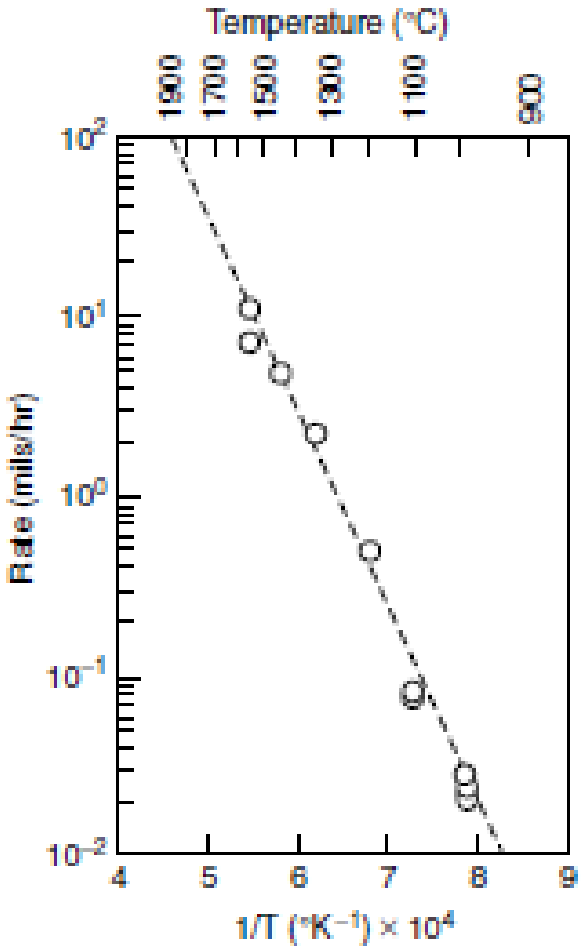

Figure 3.33 Arrhenius plot for the deposition of Si_3N_4. Reprinted, by permission, from F. Galasso, *Chemical Vapor Deposited Materials*, p. 23. Copyright © by CRC Press.

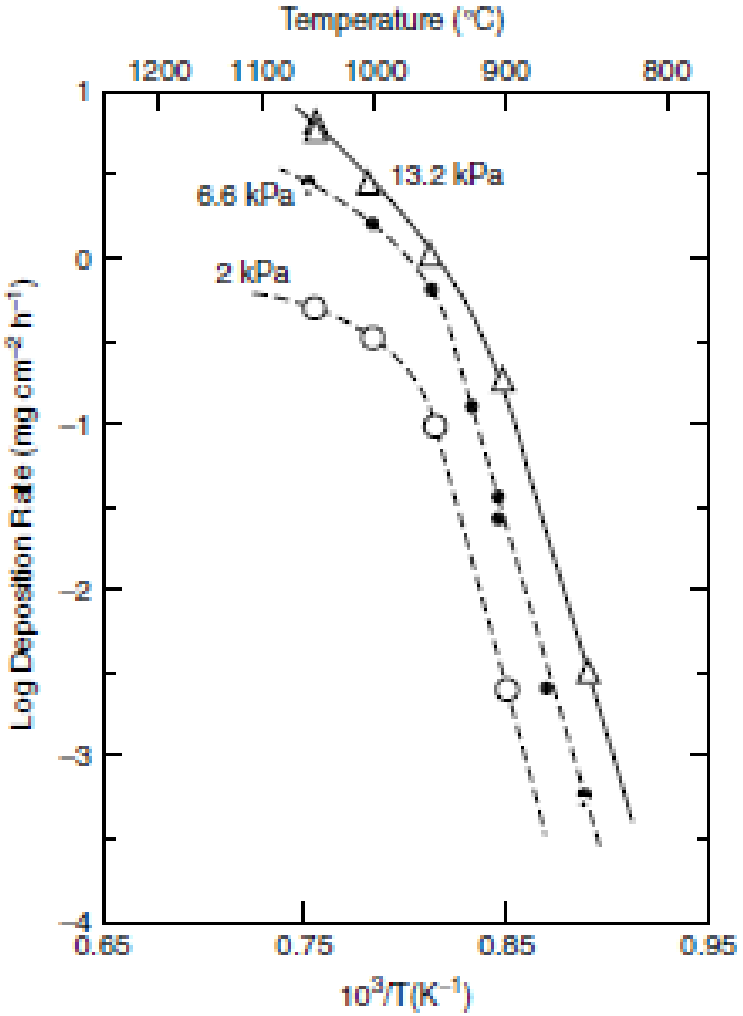

Figure 3.34 Arrhenius plot for the deposition of B_4C at various total pressures. Reprinted, by permission, from R. Naslain, CVI composites, in *Ceramic-Matrix Composites*, R. Warren, ed., pp. 199–244. Copyright © 1992 by Chapman & Hall, London.

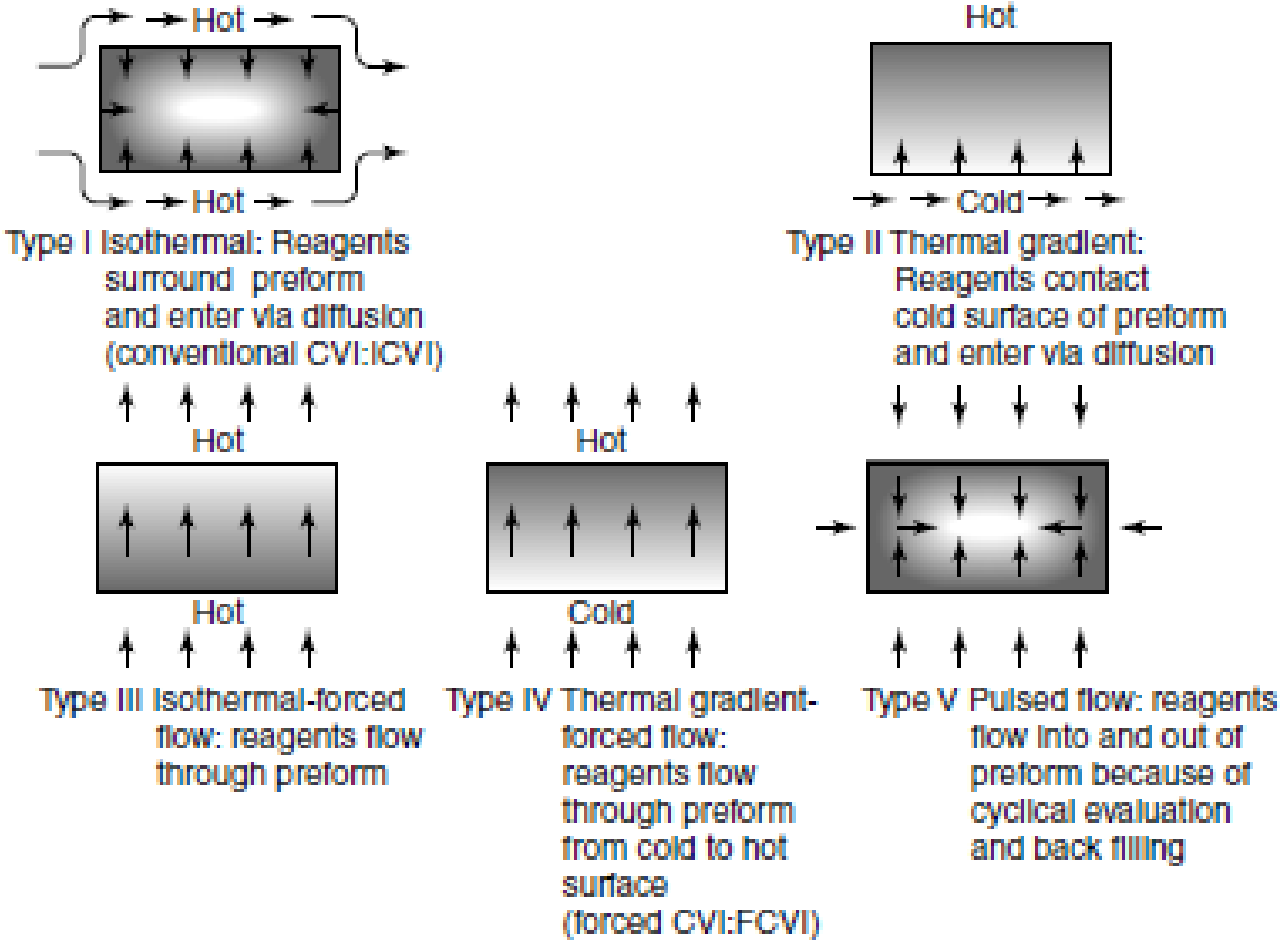

Figure 3.35 Classification of chemical vapor infiltration processes. From *Carbide, Nitride, and Boride Materials Synthesis and Processing*, A. W. Weimer, ed. p. 563. Copyright © 1997 by Chapman & Hall, London, UK, with kind permission of Kluwer Academic Publishers.

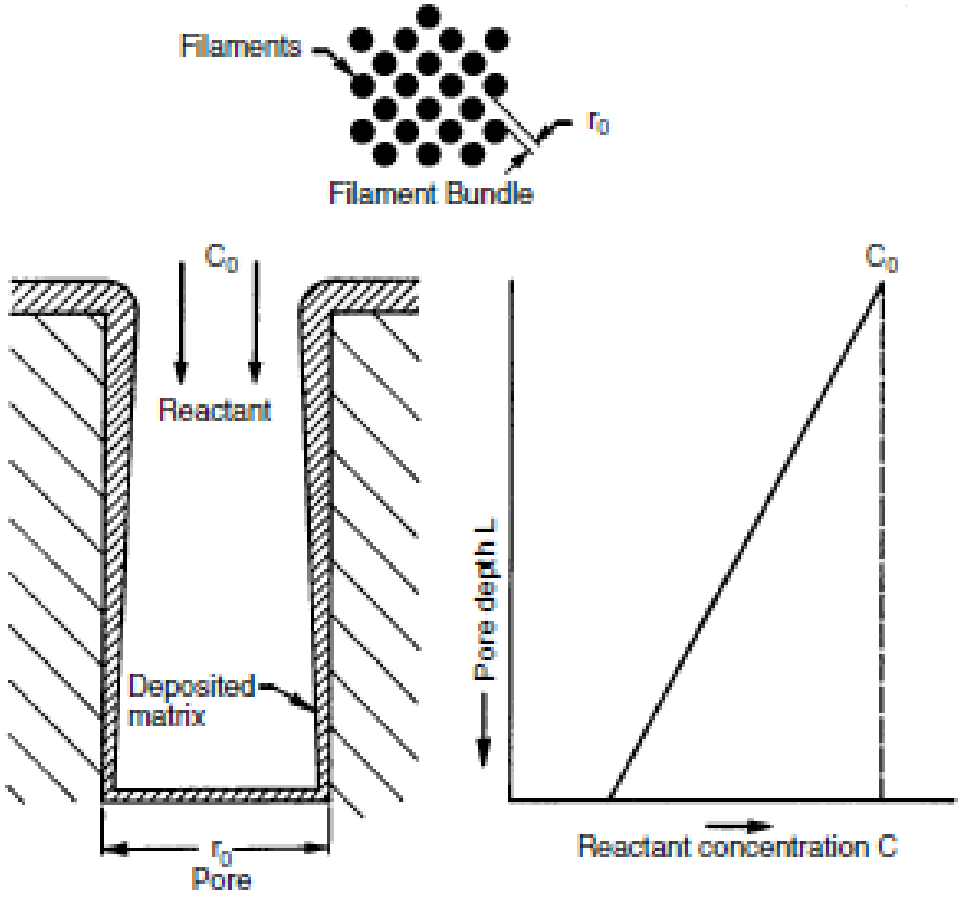

Figure 3.36 Schematic diagram of pore-filling process in the chemical vapor infiltration of a fiber bundle. From *Carbide, Nitride, and Boride Materials Synthesis and Processing*, A. W. Weimer, ed., p. 566, Copyright © 1997 by Chapman & Hall, London, with kind permission of Kluwer Academic Publishers.

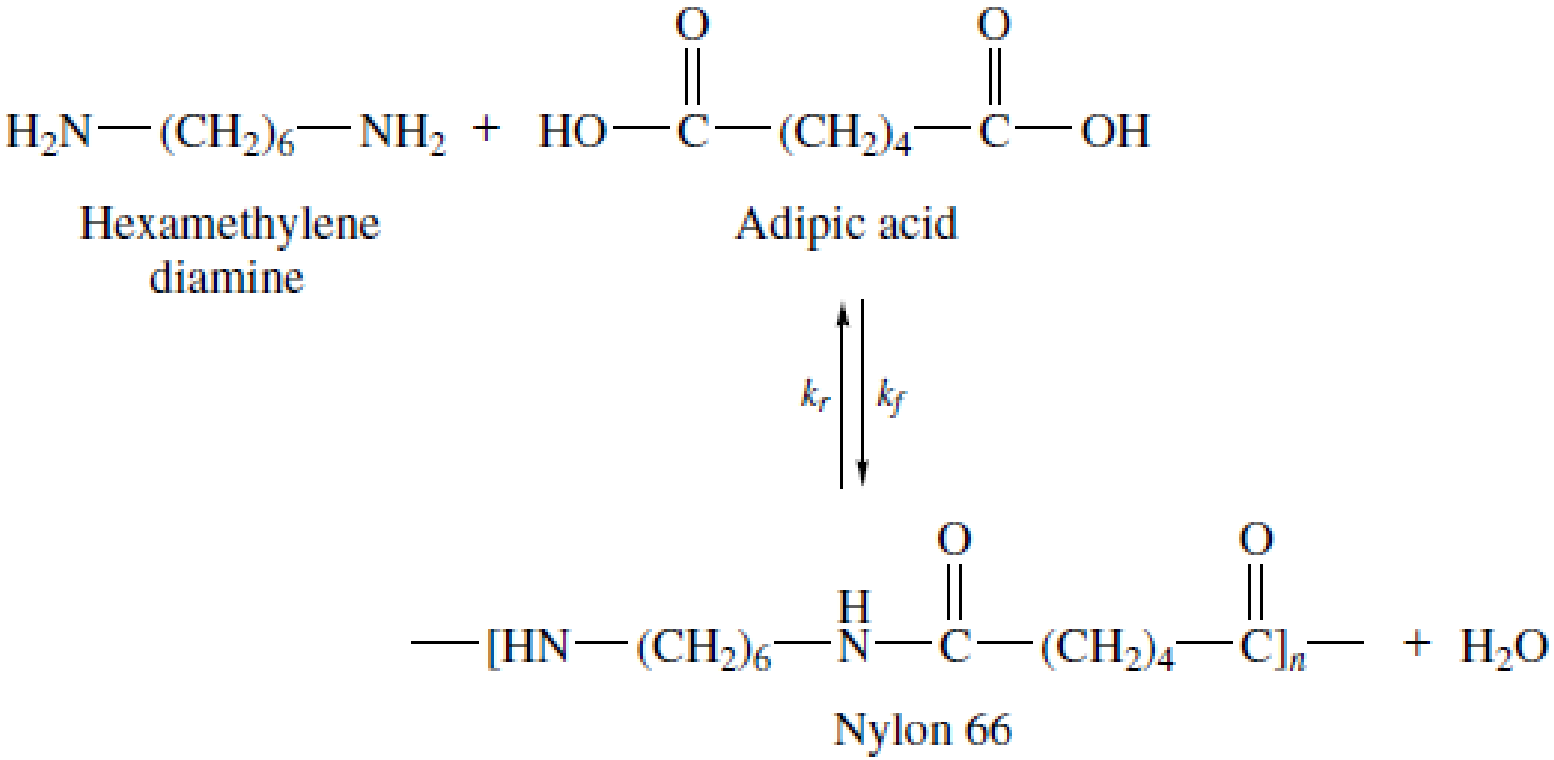
H2N—(CH2)6—NH2 + HO—C—(CH2)4—C—OH
Hexamethylene diamine
Adipic acid
kr
kf
—[HN—(CH2)6—N—C—(CH2)4—C]n— + H2O
Nylon 66

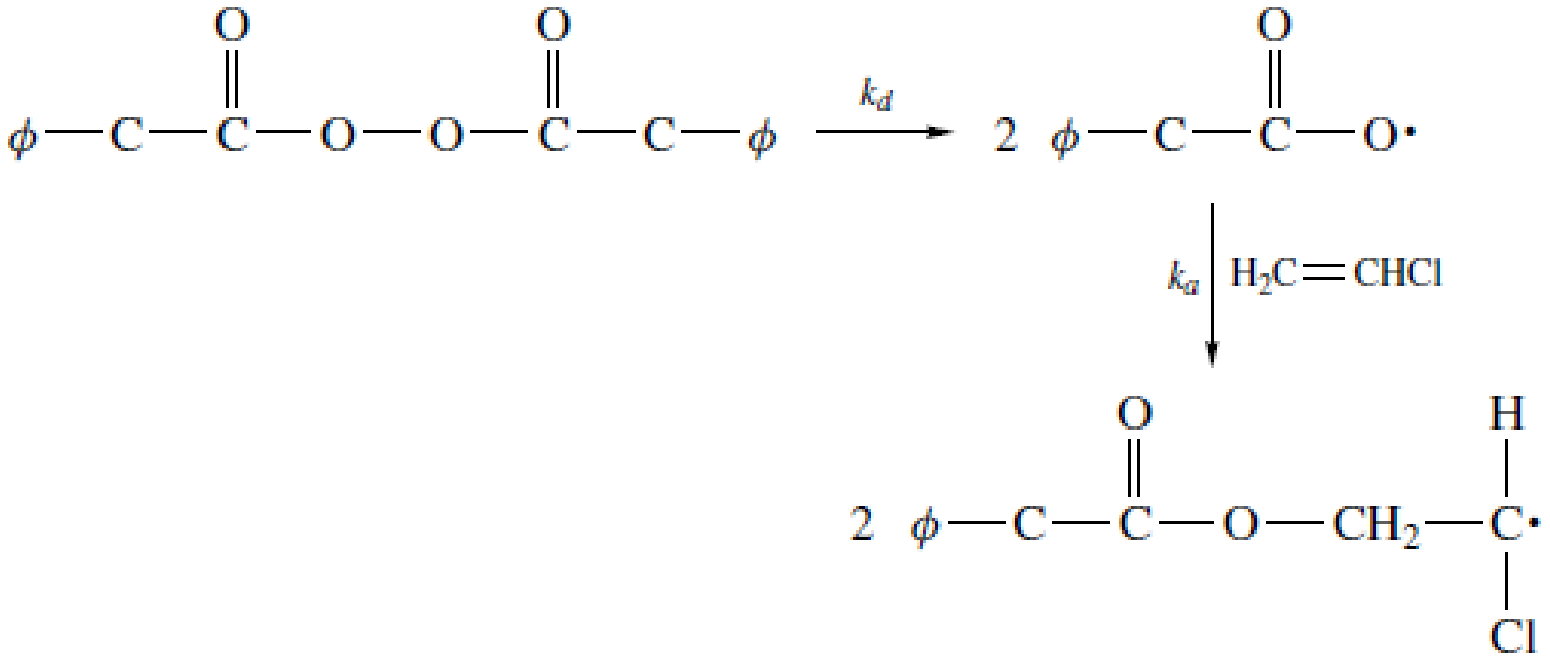
k_d
2
k_a
$H_2C=CHCl$
2

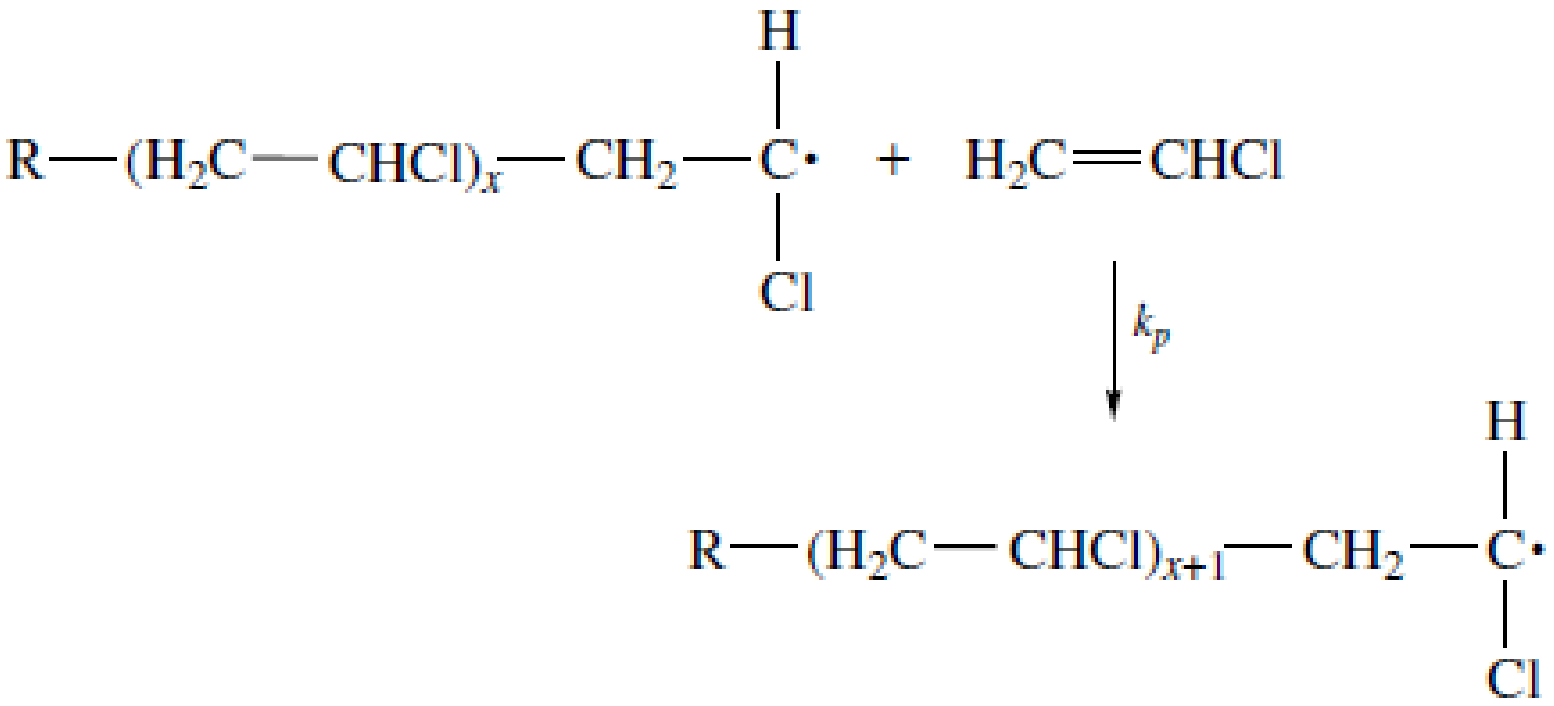
R—(H2C—CHCl)x—CH2—C•
H
Cl
+
H2C=CHCl
kp
R—(H2C—CHCl)x+1—CH2—C•
H
Cl

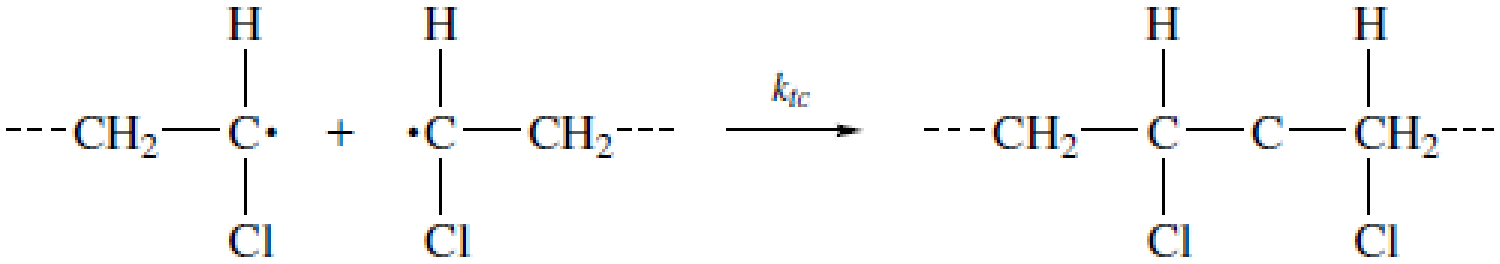

termination by combination

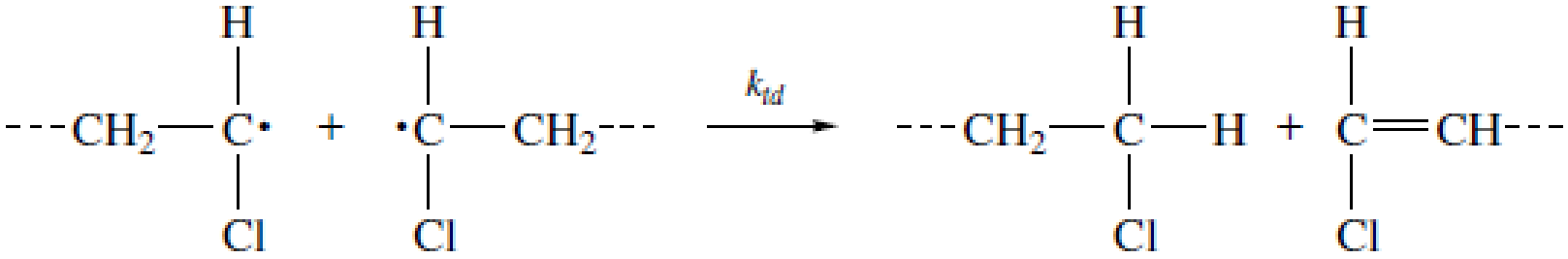

termination by disproportionation

Table 3.8 Comparison of Polymerization Processes

Type	Advantages	Disadvantages
Batch bulk	Minimum contamination	Poor heat control
	Simple equipment	Broad MW distribution
Continuous bulk	Better heat control	Requires stirring, separation, and recycle
	Narrower MW distribution	
Solution	Good heat control	Not useful for dry polymer
	Direct use of solution possible	
		Solvent removal difficult
Suspension	Excellent heat control	Requires stirring
	Direct use of suspension possible	Contamination by stabilizer possible
		Additional processing (washing, drying) required
Emulsion	Excellent heat control	Contamination by emulsifier likely
	Narrow MW distribution	Additional processing (washing, drying) required
	High MW attainable	
	Direct use of emulsion possible	

Source: Adapted from F. W. Billmeyer, *Textbook of Polymer Science*, Wiley, New York.

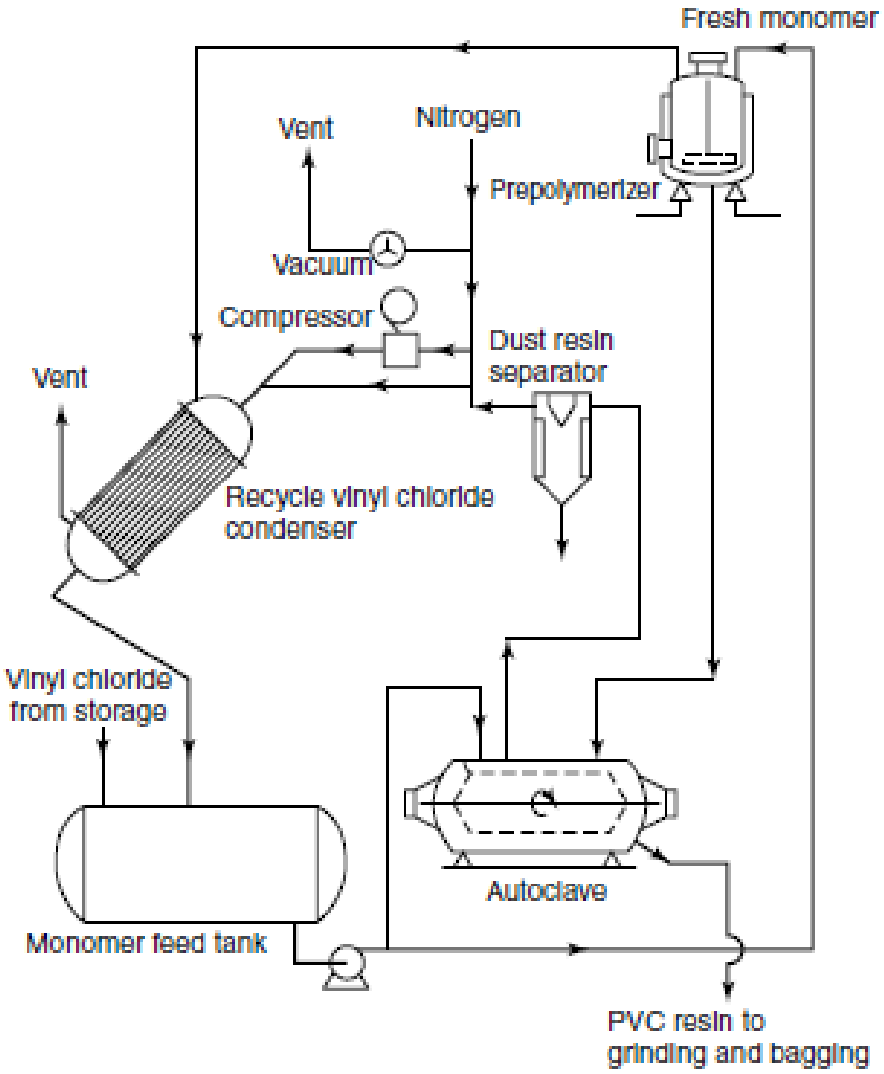

Figure 3.21 Schematic diagram of vinyl chloride bulk, continuous polymerization. Reprinted, by permission, from A. Krause, *Chem. Eng.*, **72**, p. 72. Copyright © 1965 by McGraw-Hill.

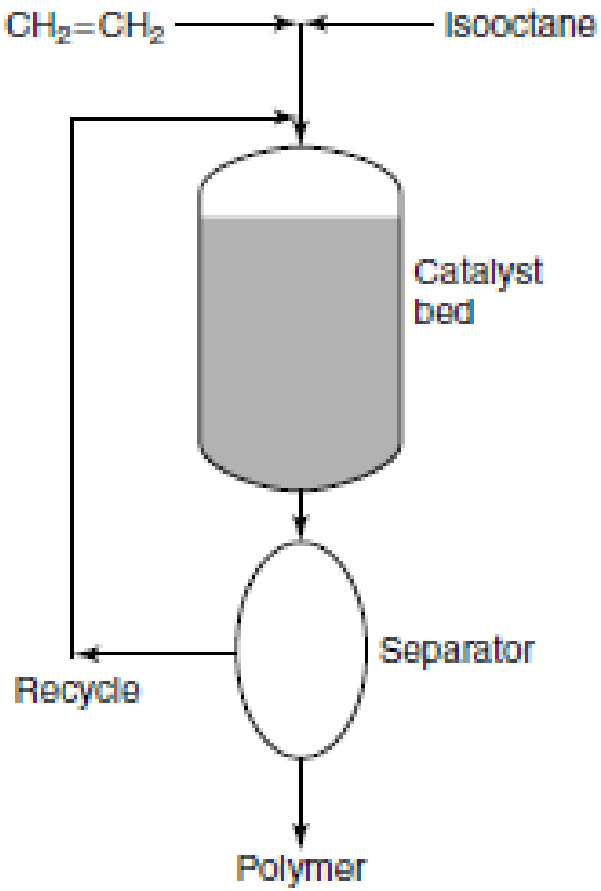

Figure 3.23 Schematic diagram of ethylene solution polymerization process.

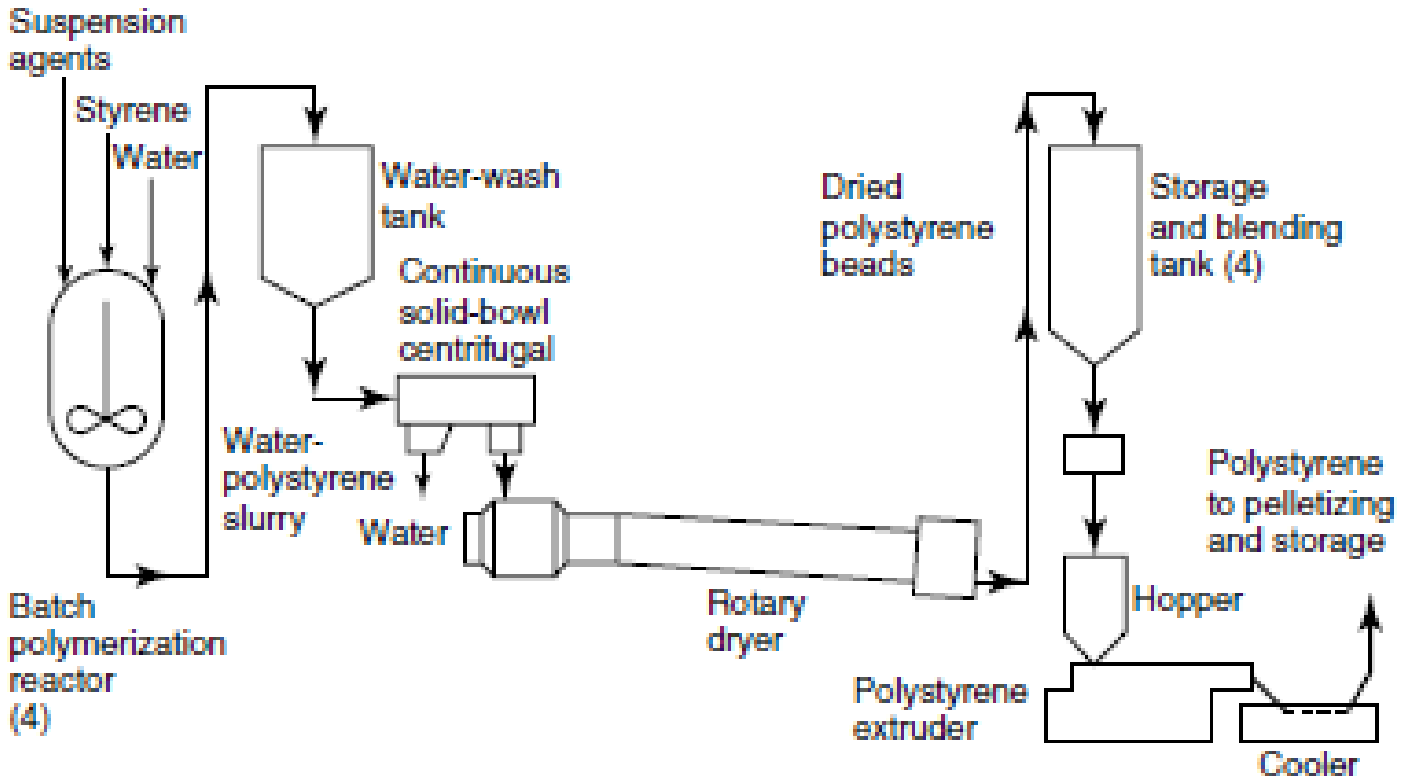

Figure 3.24 Schematic diagram of styrene suspension polymerization process. Reprinted, by permission, from *Chem. Eng.*, **65**, 98. Copyright © 1958 by McGraw-Hill.

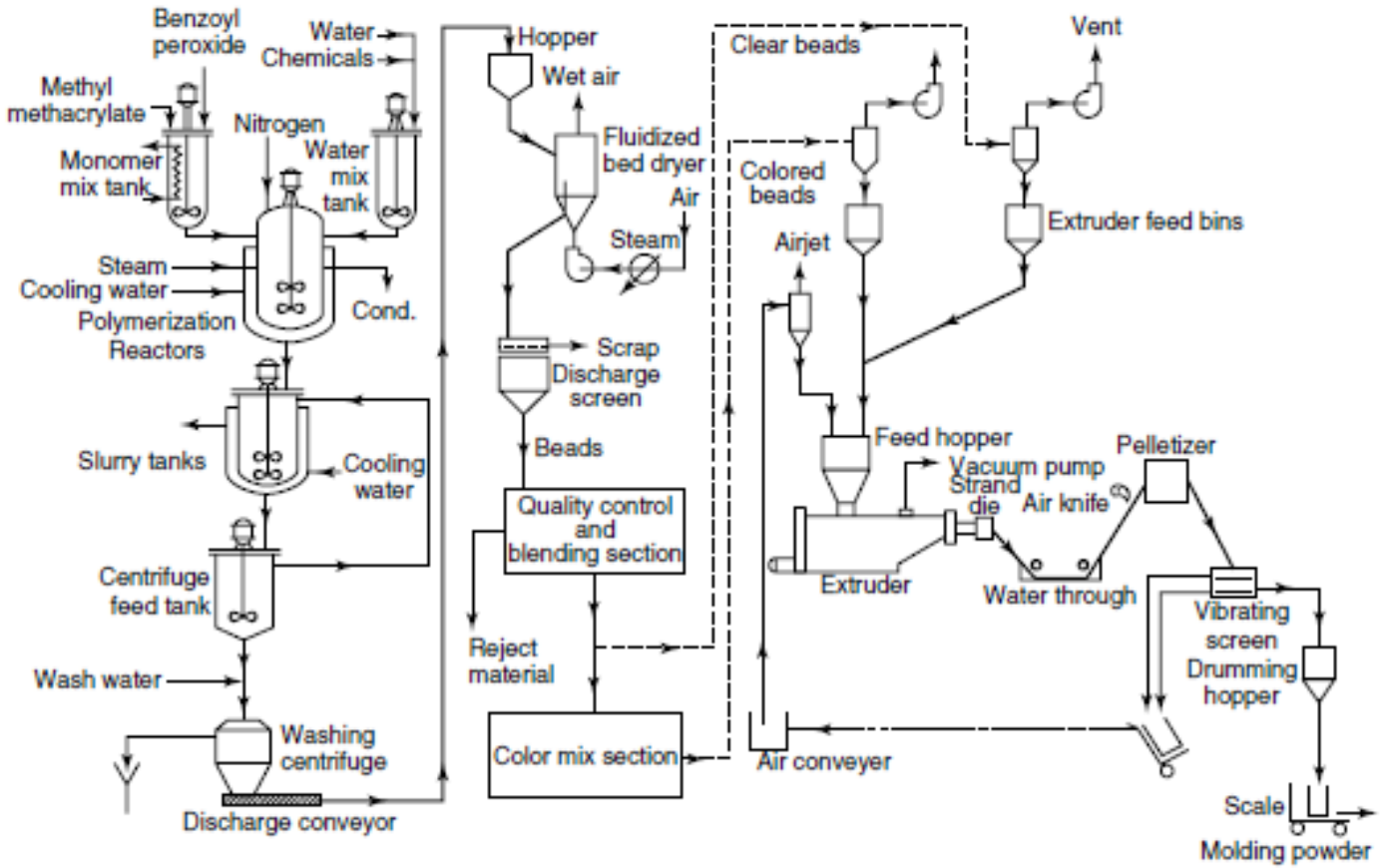

Figure 3.25 Schematic diagram of methyl methacrylate suspension polymerization process. Reprinted, by permission, from E. Guccione, *Chem. Eng.*, **73**, 138. Copyright © 1966 by McGraw-Hill.

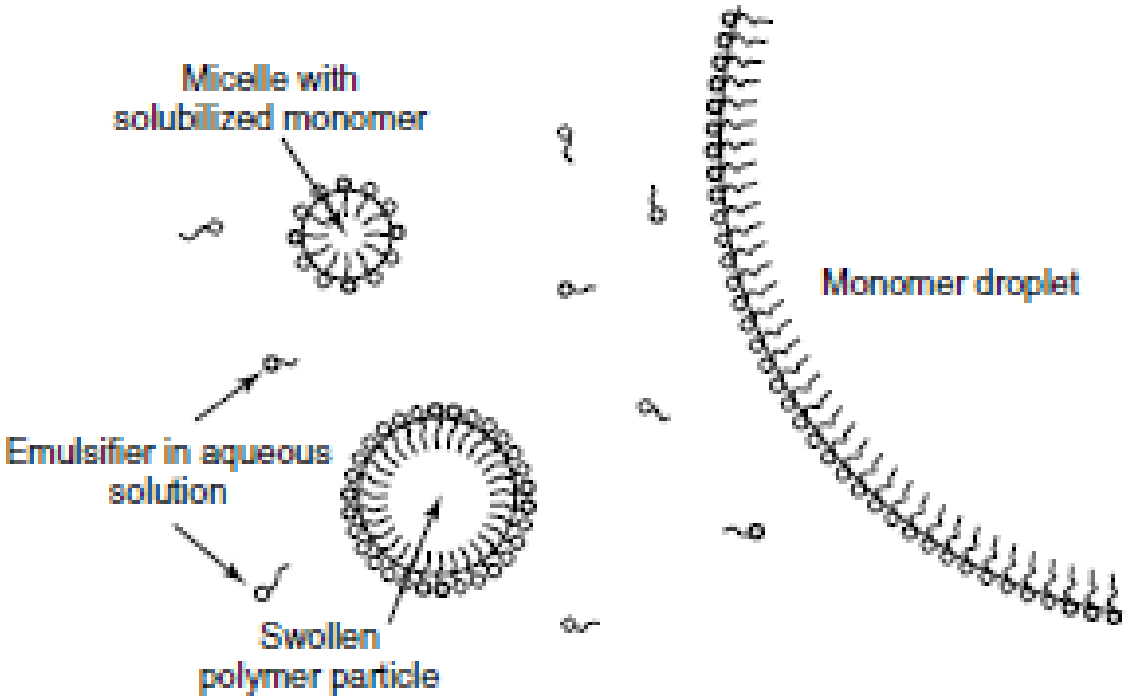

Figure 3.26 Schematic representation of micelle formation in emulsion polymerization.

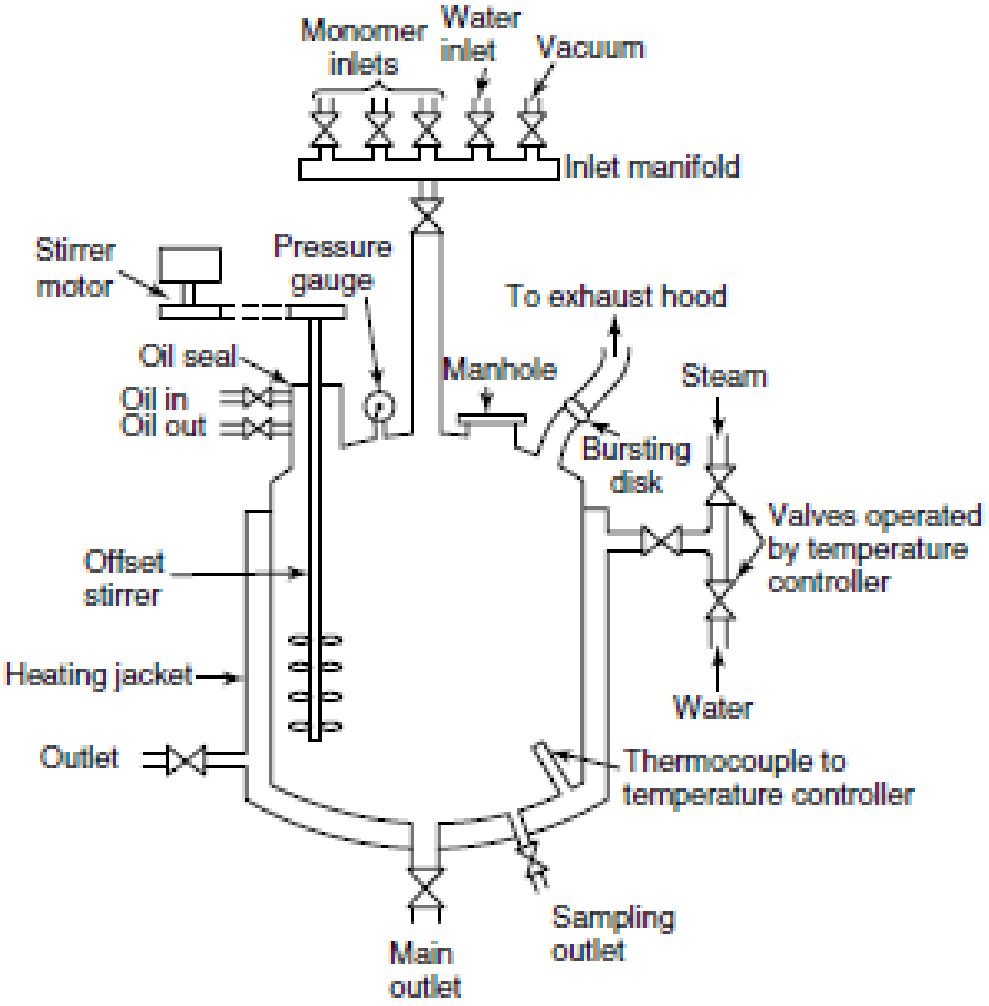

Figure 3.27 Schematic diagram of a typical emulsion polymerization reactor. Reprinted, by permission, from J. A. Brydson, *Plastic Materials*, p. 160. Copyright © 1966 by Van Nostrand.

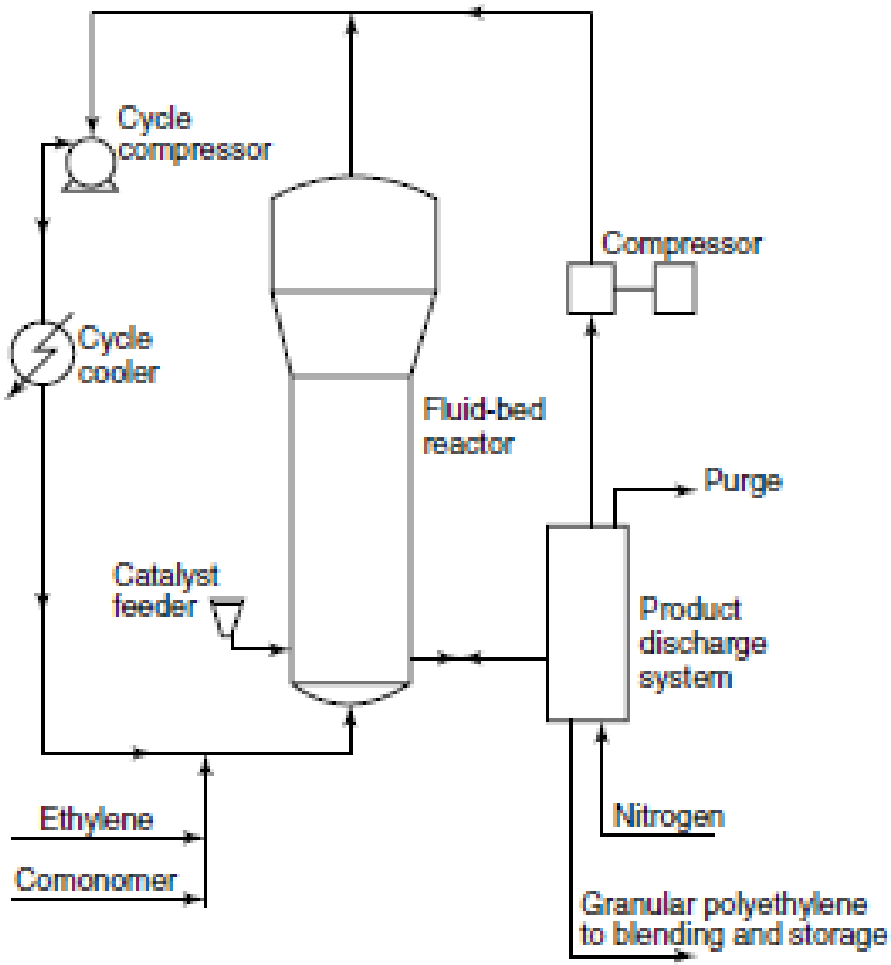

Figure 3.28 Schematic diagram of ethylene gas phase polymerization process, Reprinted, by permission, from *Chem. Eng.*, **80**, 71. Copyright © 1979 by McGraw-Hill.